

Temperature Dependence of Photoluminescence Lifetime of Rhodamine B

Heather Longstaff Hogg

A senior thesis submitted to the faculty of  
Brigham Young University  
in partial fulfillment of the requirements for the degree of  
Bachelor of Science

John Colton, Advisor

Department of Physics and Astronomy  
Brigham Young University

Copyright © 2018 Heather Longstaff Hogg

All Rights Reserved

## ABSTRACT

### Temperature Dependence of Photoluminescence Lifetime of Rhodamine B

Heather Longstaff Hogg  
Department of Physics and Astronomy, BYU  
Bachelor of Science

Determining the relationship between temperature and photoluminescence lifetime is central to creating temperature probes for microfluidic devices and laser surgery. Rhodamine B, a highly photoluminescent organic dye, is a particularly good candidate for temperature probes. This thesis discusses the use of time-correlated single photon counting to determine photoluminescence lifetimes of rhodamine B at temperatures from 16 K to 296.5 K. The instrument response function is separated from the true photoluminescence lifetime data with deconvolution data analysis techniques. The relationship between temperature and photoluminescence lifetime for rhodamine B is shown to be most accurately represented by a sigmoidal function, with very little variation at low temperature ranges. It is concluded that the behavior of the lifetime follows theoretical quenching regions over different temperature ranges.

Keywords: [TCSPC, lifetime, rhodamine B, photoluminescence]

## ACKNOWLEDGMENTS

Many thanks to my advisor John Colton for all his help in the research and proofreading, and to my husband and parents for their endless support.

# Contents

<b>Table of Contents</b>	<b>iv</b>
<b>List of Figures</b>	<b>vi</b>
<b>1 Introduction</b>	<b>1</b>
1.1 Organization . . . . .	1
1.2 Motivation . . . . .	1
1.3 Photoluminescence . . . . .	2
1.4 Rhodamine B . . . . .	4
1.5 Current Research . . . . .	4
<b>2 Experimental method</b>	<b>5</b>
2.1 Overview . . . . .	5
2.2 Time-correlated single photon counting . . . . .	5
2.3 Picoquant TCSPC card . . . . .	10
2.4 Setup . . . . .	11
2.5 Data Collection . . . . .	14
2.5.1 Calibration . . . . .	14
2.5.2 Data Acquisition . . . . .	16
2.6 Issues Encountered . . . . .	17
<b>3 Results and Conclusions</b>	<b>18</b>
3.1 Overview . . . . .	18
3.2 Deconvolution . . . . .	18
3.3 Data . . . . .	20
3.4 Conclusions . . . . .	24
3.5 Further Work . . . . .	24
<b>Appendix A TCSPC Settings</b>	<b>25</b>
<b>Appendix B PID Controller</b>	<b>27</b>
<b>Appendix C Data Analysis Code</b>	<b>29</b>

<b>Index</b>	<b>33</b>
<b>Index</b>	<b>33</b>
<b>Bibliography</b>	<b>34</b>
<b>Index</b>	<b>36</b>

# List of Figures

1.1	Photoluminescence . . . . .	3
2.1	Setup of standard TCSPC modules. From Ref. [1]. . . . .	6
2.2	Statistical representation of photoluminescence lifetime . . . . .	7
2.3	Common fraction discriminator . . . . .	8
2.4	Zero cross level . . . . .	8
2.5	Setup of Picoquant PICO module. From Ref. [2]. . . . .	10
2.6	Setup for measuring RhB lifetime. . . . .	11
2.7	Pulse generator delay time . . . . .	12
2.8	RhB data with multiple excitation peaks . . . . .	13
3.1	One PL lifetime decay curve for rhodamine B at 296.5 K. . . . .	19
3.2	One IRF decay curve at 296.5 K. . . . .	19
3.3	Photoluminescence lifetime vs. temperature fitted with a sigmoidal function for rhodamine B . . . . .	21
3.4	Five-parameter sigmoidal fits with RhB PL lifetime data. The fits are extended beyond the measured temperatures to 800 K. The fitting parameter b is forced to 1 ns, 2 ns, and 3 ns. Only the inflection point and the minimum asymptote vary. . .	22
3.5	Photoluminescence spectra plotted at the measured temperatures. . . . .	23

# Chapter 1

## Introduction

### 1.1 Organization

The purpose of this thesis is to determine the relationship between the photoluminescence lifetime of rhodamine B (RhB) and temperature. In this chapter, I will discuss the importance of this research and why RhB was selected. In chapter 2, I will review my experimental setup, time-correlated single photon counting, and taking data. In Chapter 3, I will examine the results of the experiment, data analysis, and discuss further work and application.

### 1.2 Motivation

Photoluminescent materials are heavily studied because of their vast range of potential uses in modern technology. In particular, they can be used as temperature sensors in situations not suited for conventional thermometers. Paviolo et al. discuss that in the rising field of microfluidic devices these photoluminescent materials can be used to monitor the temperature of chemical reactions and medical or biological tests inside microscale fluid channels [3]. In photothermal therapy and neural prosthetics, which require high energy lasers, they can be used to monitor the temperature

of surrounding tissue and help prevent excessive heat damage. Using photoluminescent materials as temperature sensors does not require direct contact with external equipment, making them particularly useful in sterile environments [3].

### 1.3 Photoluminescence

Photoluminescence (PL) is the process of an excitation of an electron in a photoluminescent material and subsequent emission of a photon. The PL process in chemical dyes, such as rhodamine B, begins when the material is excited by a high energy photon and the photon energy is transferred to an electron in the highest occupied molecular orbital (HOMO). The electron is excited into a high-energy state in the lowest unoccupied molecular orbital (LUMO). Over time, the electron releases energy through non-radiative processes, such as heat and vibrations, and moves down to the bottom level of the LUMO. At this point, the electron recombines back into the HOMO and releases excess energy as a PL photon. Fig. 1.1 represents the PL process visually. Because the emitted PL photon is characterized by the difference in energy between the LUMO and HOMO, each PL photon will have nearly the same energy, which is determined by the material. The corresponding wavelength, defined as  $\lambda = hc/E$ , is the PL wavelength.

Two of the most important properties of PL are lifetime and intensity. The excited electron loses energy over time in non-radiative properties and eventually recombination and emission. This delay between initial excitation and the emission of a PL photon is the PL lifetime of the material. Photoluminescence intensity is the number of emitted photons. In many cases, both PL intensity and lifetime depend on temperature.

Because many photoluminescent materials exhibit temperature dependent PL intensities and lifetimes, both can be used to measure temperature. However, PL lifetime has the potential to be superior over PL intensity in accurately measuring temperature, as PL intensity is dependent on

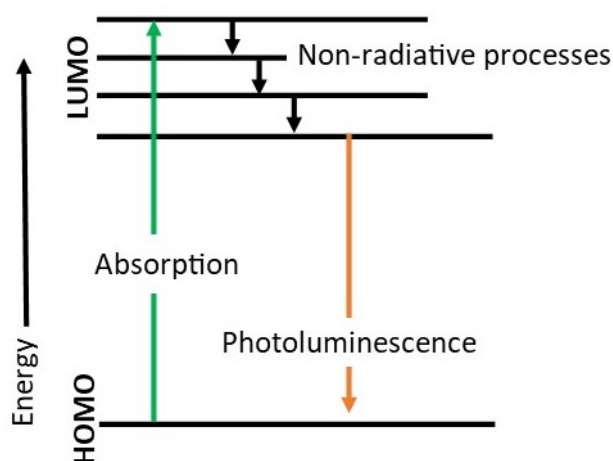


**Figure 1.1** Diagram of PL process. Electrons are excited by an excitation photon. Over time they recombine with the highest occupied molecular orbital and emit a PL photon.

the concentration and number of particles in the sample, background light, and the strength of the excitation light source [3]. This dependence makes using PL intensity as a temperature probe virtually impossible outside of a well-regulated laboratory setting and make the results difficult to replicate. Photoluminescence lifetime, however, is only dependent on the type of material used, meaning the results should be able to be replicated and accurately measured in any setting [3]. Because of this, PL lifetimes of different materials can be documented in advance and used as a reference for determining temperature. This thesis will report the photoluminescence lifetime and temperature relationship for the well-known dye rhodamine B (RhB) for future reference for RhB temperature probes.

An important parameter of PL is the quantum yield, or the number of photons emitted vs. the number of photons absorbed. Intensity of the PL emission and PL lifetime are determined by the quantum yield. Quantum yield can be reduced by quenching, a process that interferes with the emission of a photon and occurs during the PL lifetime. In dynamic quenching, a molecule such as oxygen must be in direct contact with the material and will prevent photon emission in

different ways depending on the quencher [4]. The quantum yield ratio improves towards one, or perfect efficiency, as temperature decreases and high temperature quenching effects are less likely to reduce the efficiency of emission [4–6]. Photoluminescence lifetime is affected by the quantum yield of the sample, so it is important to prevent quenching effects from artificially reducing the photoluminescence lifetime.

## 1.4 Rhodamine B

Rhodamine B is a fluorophore, or a chemical compound that exhibits photoluminescence. It is common in biology and chemistry due to its relatively high quantum yield, making it easy to detect [7]. Photoluminescence lifetime and intensity of RhB are both temperature dependent, unlike some other dyes in the rhodamine family. This dependence has been attributed to the flexible rotating bonds of the chemical structures attached to the xanthene base [8]. The lifetime of RhB is dependent not only on temperature, but also on the chemical environment of the solvent, including pH and viscosity [9, 10].

## 1.5 Current Research

Rhodamine B is common in current biological and chemical work, so lifetime and temperature dependence has been well-documented. In a technical note from the company Edinburgh Instruments, RhB PL lifetime is measured from 278 K to 353 K in water [5]. Other temperature vs. lifetime measurements have been done in glucose and lactose solutions, as well as alcohol solvents at temperatures between 273 K and 373 K [9, 11]. Both these results, and others, report the lifetimes to be between 0.4 ns and 2.5 ns. However, there is very few, if any, measurements of RhB PL lifetime below 300 K. This thesis will focus on the low temperature lifetime of RhB that has been allowed to dry inside a channel in resin and is independent of a solvent.

# Chapter 2

## Experimental method

### 2.1 Overview

In this chapter, I will explain time-correlated single photon counting (TCSPC) along with important considerations associated with it, including common fraction discriminator, dead time, pile-up, forward and reverse modes, and the instrument response function. I will outline the experimental setup, discuss how data was taken, and examine a few issues encountered.

### 2.2 Time-correlated single photon counting

Time-correlated single photon counting is a technique used to determine PL lifetime (the time in between excitation and recombination of an electron) via the detection of individual photons. The basic principle is the same in every TCSPC system, although acquisition specifics may differ. Every TCSPC system needs three things: a reference pulse from a pulsed laser, a detected PL photon, and a stopwatch which measures the time between the reference pulse and the PL photon. The stopwatch is typically housed in a peripheral component interconnect (PCI) module that works with TCSPC software.

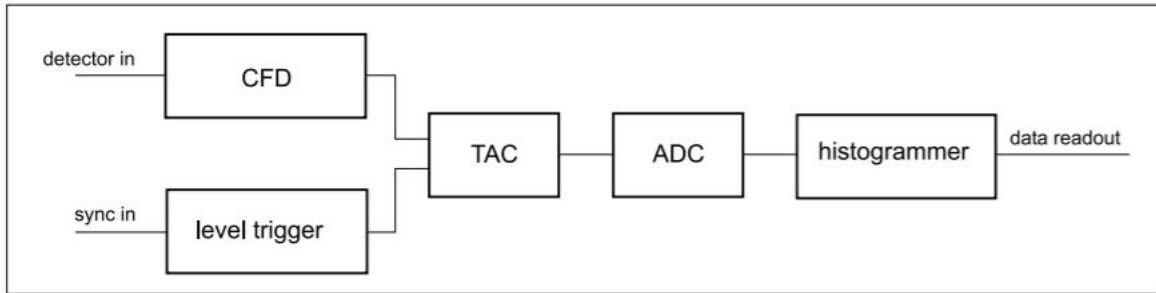
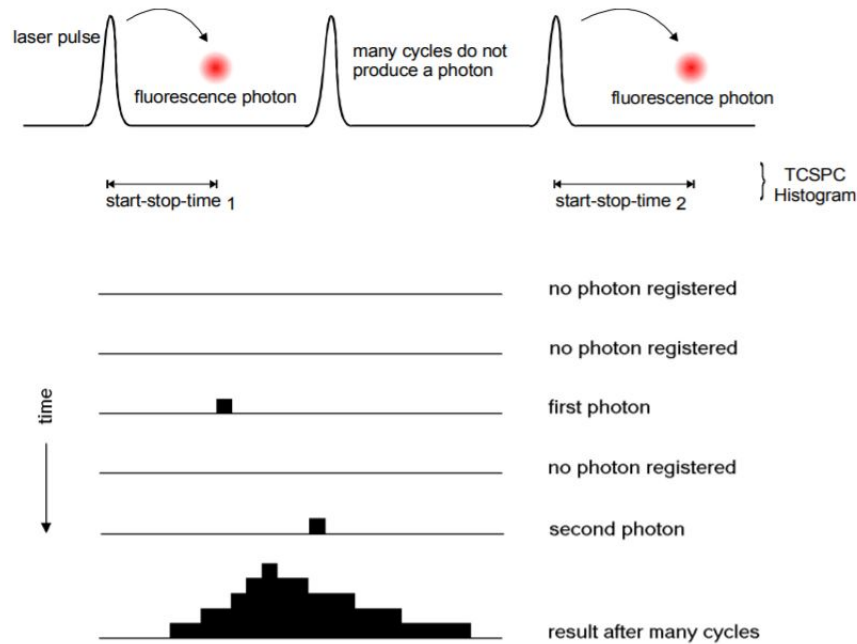


**Figure 2.1** Setup of standard TCSPC modules. From Ref. [1].

The TCSPC module works by first receiving the laser reference pulse, which triggers the module to start charging a capacitor. The capacitor charges until the PL photon is received, and the amount of charge stored is converted into time via a time-to-amplitude converter (TAC), and then into a readable format via an analog-to-digital converter (ADC), as shown in Fig. 2.1. Fig. 2.2 shows the buildup of this process over thousands of photon measurements. Each recorded photon is added to a histogram of number of counts vs. the time delay as a statistical representation of the photoluminescence lifetime.

Time-correlated single photon counting is a theoretically simple process. However, TCSPC in practice proves to be much more complicated, as imperfect and inefficient electronic components are introduced, as well as samples that do not produce only one photon at a time. It is therefore important to understand the limitations and corrections in TCSPC and be able to control data collection for accurate PL lifetimes.

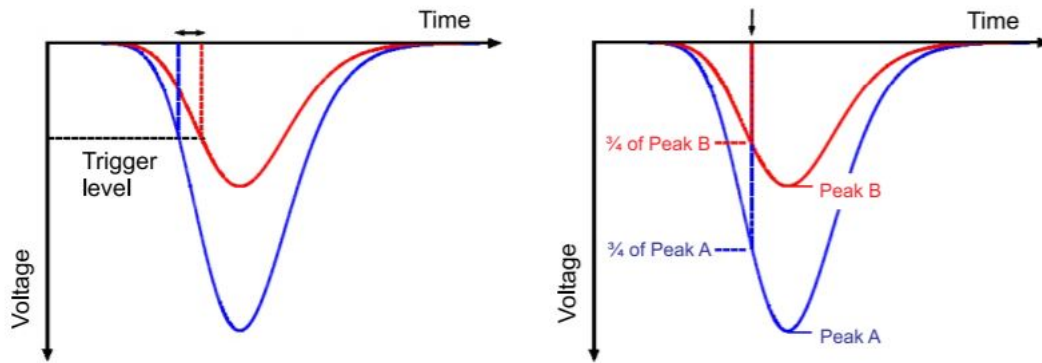
One of these considerations is the need for a common fraction discriminator (CFD) to provide accurate timing. The amplitudes of PL photon pulses from a photon detector are often not consistent. Variation in each pulse is not easily ignored, as it may lead to incorrect timing of the photon, as shown in Fig. 2.3. A voltage threshold level is defined in TCSPC to discriminate between small noise pulses and pulses triggered by a PL photon, but this can be inaccurate. A CFD uses a fraction of the amplitude, instead of the set threshold level, to determine when the pulse is counted. As in



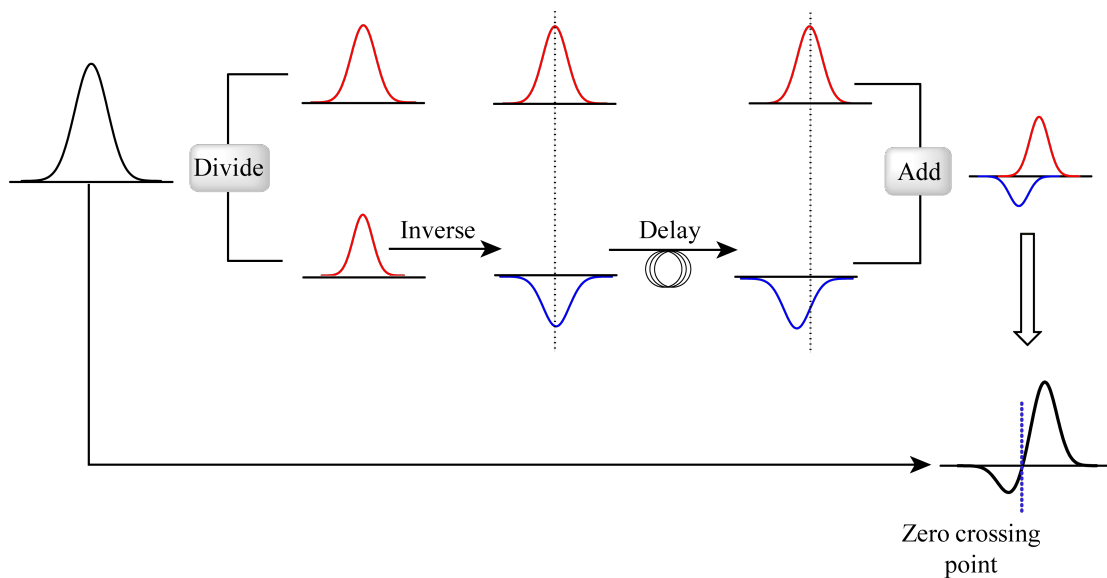
**Figure 2.2** Building a histogram with TCSPC. Each detected photon contributes to a statistical representation of the lifetime. From Ref. [2].

Fig. 2.3, this allows the timing of each detection of a photon to be consistent, regardless of pulse height. Part of the CFD is the zero crossing level, which determines at which point the pulse is accepted. As shown in Fig. 2.4, the CFD sends the pulse through two paths: first, the pulse is sent unaltered through a gate that determines if it passes the set threshold amplitude; second, it is multiplied by a constant fraction to reduce the amplitude, and inverted. The two resulting pulses from these paths are added together and the point at which the resultant function passes through zero is the zero crossing point, which becomes the time at which the pulse is accepted.

Another of the most important considerations in TCSPC is dead time. When a start pulse is received, the capacitor will begin to charge; if there is no stop pulse, the capacitor will eventually reach a limit and will have to reset. This reset takes time, during which no other start pulse will be able to be recorded. This is dead time. If the stop pulse is received, then the dead time also includes the conversion and processing of the measured time. Dead time is usually significant enough that



**Figure 2.3** A common fraction discriminator reduces timing error in TCSPC. It accepts a pulse based on fraction of amplitude, rather than a set voltage level. From Ref. [1].



**Figure 2.4** A visual description of how the zero cross level is calculated. The pulse is added to an inverted fraction of itself to determine the time at which the pulse is counted. From Ref. [12].

many PL photons will be lost. This increases the necessary data acquisition time. It is also the reason that TCSPC cards do not record more than one photon per start pulse [1]. The consequences of this are most noticeable in the pile-up effect.

The pile-up effect is a source of misrepresentation of the PL lifetime. Because of the effects of dead time, the PL photon detector should only receive one photon per laser excitation pulse. If two or more photons reach the detector during this time, they will not be recorded, as the TCSPC card is busy processing the first. Over time, the statistical representation of the lifetime will be skewed to favor the "faster" photon, giving inaccurate data. The most effective way to combat this photon pile-up is to attenuate the PL photon counts down to less than one percent of the laser reference frequency, i.e. only one PL photon for every 100 laser pulses. This will guarantee accurate measurements.

A third consideration is forward mode vs. reverse mode. Most TCSPC cards will work in one or both of two ways: forward or reverse mode. Forward mode is the method previously described, where the laser reference pulse starts the timing process. However, this method is often inefficient. When PL photons are attenuated down to less than one percent of the reference pulse, the timer will be constantly started, but stopped relatively rarely. The TCSPC card will have to reset many times without recording data, resulting in significant amounts of dead time during which many photons may be unrecorded [1]. Most cards will address this by using a reverse mode, where the PL photon starts the timer and the next laser pulse stops it. The resulting plot is then reversed on the time axis to generate a plot consistent with forward mode. In reverse mode, the timer is only started when there is data to be recorded, rather than triggering off useless pulses and losing excessive photons due to dead time.

The last consideration for TCSPC is the instrument response function (IRF). Raw data for TCSPC sample measurements is not accurate. The photon detector, usually a photomultiplier tube or an avalanche photodiode, does not have a infinitely fast response to an incoming photon and will thus contribute its own "lifetime" in such a way that the measured PL lifetime is a convolution of the actual PL lifetime and the detector response. This response, called the instrument response function, must be measured and removed from the data with deconvolution data analysis.

## 2.3 Picoquant TCSPC card

This experiment relied on a TCSPC card from Picoquant, a PICO model TimeHarp 260. The timing resolution for the card is 25 ps, meaning the histogram has a time bin every 25 ps. This high resolution is due to its unique layout, which is different from most TSCPC cards. As shown in Fig. 2.5, the card skips the traditional TAC and ADC route, and instead uses a time to digital converter (TDC) for each input pulse. Bypassing much of the work and converting each start and stop pulse separately speeds up the acquisition time and minimizes dead time to allow for picosecond resolution. This also allows the card to be run efficiently in forward mode [2]. Settings and safe voltage levels for the TimeHarp 260 is given in appendix A.

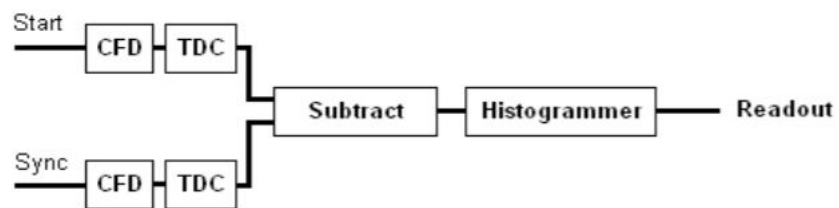


**Figure 2.5** Setup of Picoquant PICO module. From Ref. [2].

## 2.4 Setup

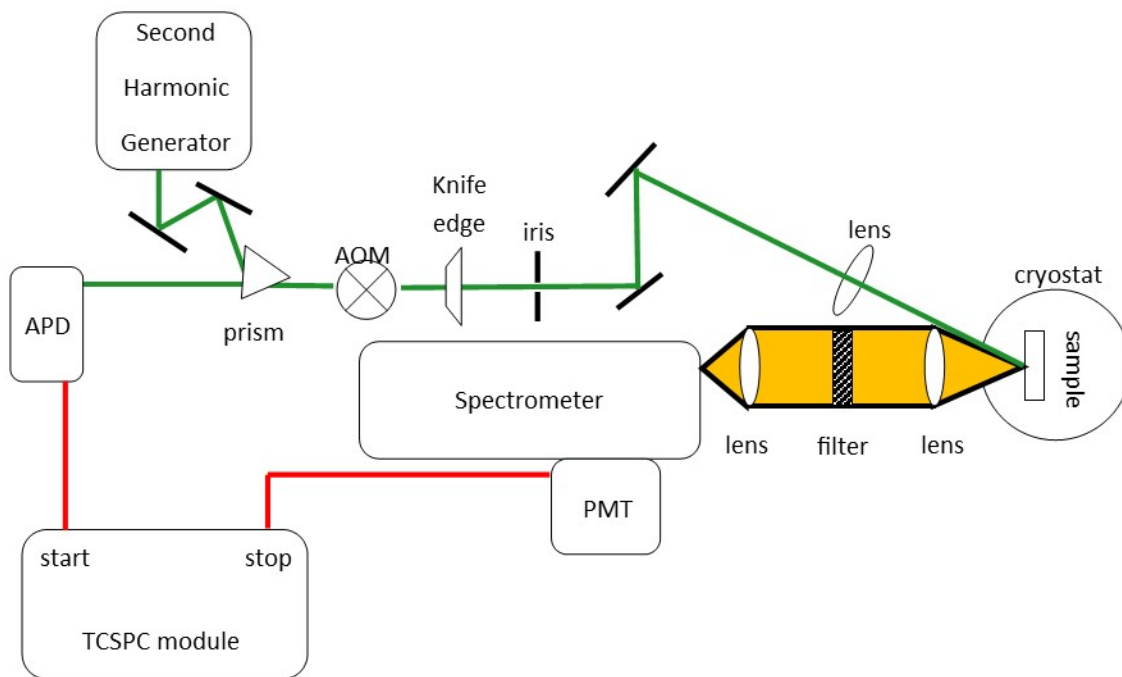


**Figure 2.6** Setup for measuring RhB lifetime.

The experimental setup used is shown in Fig. 2.6. A Tsunami 80 MHz pulsed Ti:Sapph laser was tuned to 1000 nm and the output was sent through a second harmonic generator to produce a 500 nm beam with 30 mW power to excite the sample, which photoluminescences at 583 nm. The wavelength 500 nm was chosen for excitation to bypass the 460 nm PL of the resin sample holder containing the RhB. The 500 nm beam was sent through a prism which split the beam into two beams via reflection. The main component of the beam continued to the sample, and the lesser component triggered an avalanche photodiode (APD), triggering a pulse generator which supplied the needed laser reference pulse. As can be seen in Fig. 2.6, the main beam was focused into an

acousto-optic modulator (AOM), collimated, and sent through an iris to cut off the higher order peaks. A knife edge was also placed in front of the iris to block the zeroth order peak. The first order beam was then focused onto the sample in the cryostat. The photoluminescence and laser light were scattered off the sample and collected by a collimating lens. The photoluminescence was then focused into the spectrometer which selected the desired wavelength range and directed the beam into the photomultiplier tube (PMT), which detected individual PL photons and provided the stop pulse.

This setup also made use of a pulse generator to allow many recorded excitations before stopping the TCSPC module. To do this, the APD output triggered the pulse generator, which output a -150 mV pulse to the TCSPC module to mimic the laser. A time delay was set on the pulse generator output to change the frequency of the simulated laser pulse and collect multiple decay peaks for more accurate lifetime representation. An example of a delay is demonstrated in Fig. 2.7

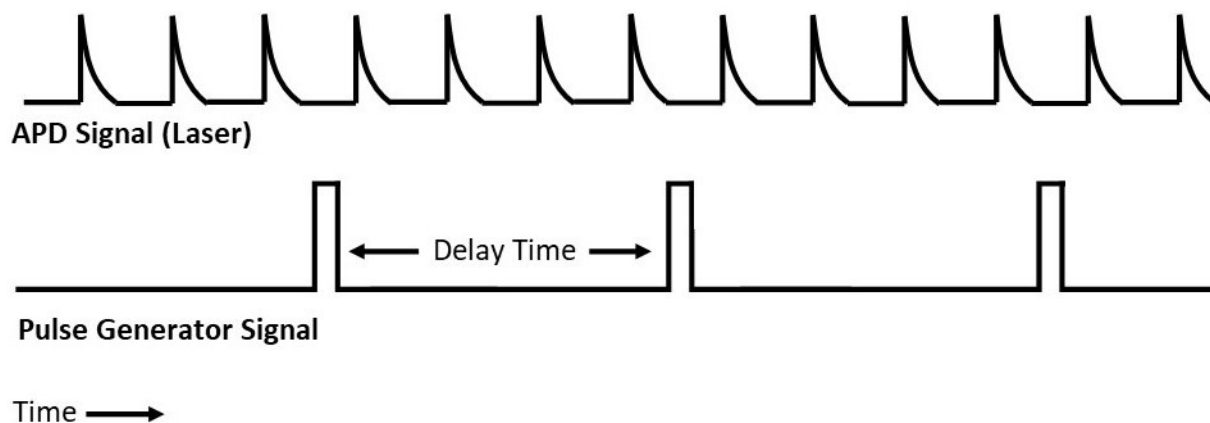


**Figure 2.7** Example timing diagram of APD and pulse generator pulses. The pulse generator is given a delay time after triggering from a laser pulse. The pulse generator sends a stop pulse to the TCSPC module at a lower frequency.

Fig. 2.8 shows some representative data collected by the TCSPC card for rhodamine B, with each start pulse given by the pulse generator allowing eight excitation peaks in the data. Multiple peaks allow averaging lifetime in data analysis for more accurate lifetime measurements.

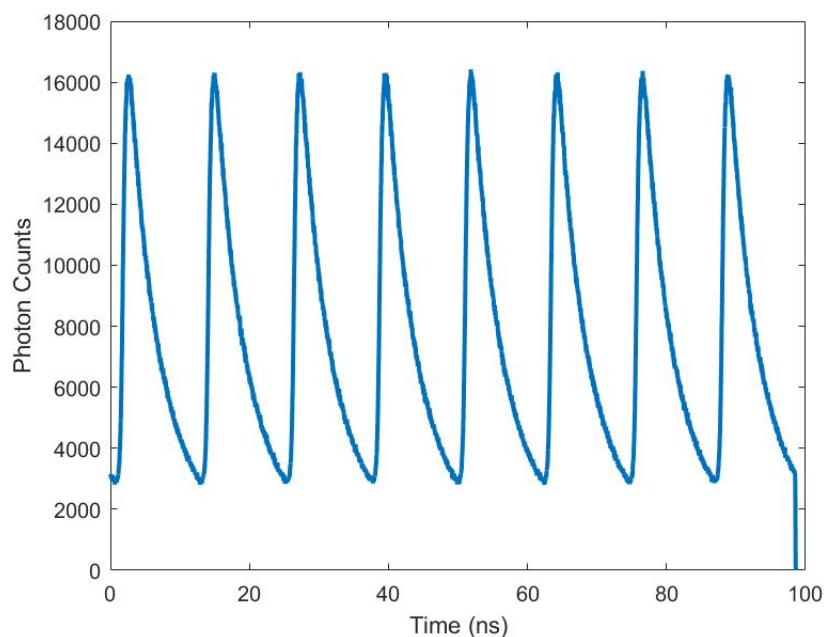


**Figure 2.8** Representative lifetime plot for RhB at 296.5 K. The pulse generator sends the TCSPC card a start signal at a lower frequency than the true laser signal, allowing multiple peaks to be recorded between start signals.

The PMT used to detect individual PL photons is water cooled to reduce dark counts to below 20 counts per second and guarantee higher precision in lifetime measurements. The input hose is pushed onto the sink nozzle and the output is left to drain into the sink. Care must be taken to avoid high pressures that may damage the PMT when using water cooling. It was also necessary to ensure adequate attenuation of the PL and laser light via neutral density (ND) filters and narrow entrance slits into the spectrometer to avoid overexposing the PMT above 10 million counts per second.

Several ND filters were used in the setup, one of which is shown in Fig 2.6, marked "filter". An ND filter is placed in the collimated PL beam to attenuate the photon counts and protect the PMT from counts above 10 million. Another ND filter is placed either in front of the APD for the sample lifetime measurements or in front of the output of the second harmonic generator for IRF measurements. With the ND filter at the output of the second harmonic generator, it will both

attenuate the high photon counts of the IRF and protect the APD.

Temperature was controlled by first securing the sample on the cold finger of a closed cycle helium cryostat with aluminum tape. Temperature was detected by a calibrated diode at the top of the cold finger. The diode was also connected to a PID-controlled heater located at the top of the cold finger, which maintains the set temperature. The settings and instructions for the PID controller at different temperatures can be found in Appendix B.

The AOM in this experiment served mainly as an attenuator. In previous and future TCSPC experiments, the AOM can be triggered by the pulse generator to shut off periodically, effectively blocking the laser beam from reaching the sample. This is useful when measuring long lifetimes (a significant portion of or longer than the time between laser pulses). Cutting off the laser during a TCSPC measurement allows the PL lifetime to decay fully without being re-excited by the laser. However, RhB PL lifetime is not a significant portion of the time between laser pulses, and the AOM was kept on at all times with a constant voltage source to attenuate the laser power. After attenuation through the AOM and iris, the final laser power exciting the sample was 1 mW.

## 2.5 Data Collection

### 2.5.1 Calibration

Correct values for TCSPC settings are vital in order to collect accurate and efficient data. The important values to consider are the zero cross, the discriminator level, the sync divider, and the offset. All these values are chosen based on the amplitude of the pulses from the sync (laser reference) source and the PMT, and from the time delay caused by information traveling through lengths of wire. The zero cross and discriminator level settings determine which pulses are processed and which are considered noise. The offset shifts the data in time to prevent the data from being cut off in the middle of the decay. The sync divider effectively divides the laser reference pulse

frequency in half, quarter, or eighth to guarantee that the TCSPC card will not receive a rate larger than the 40 MHz it can effectively handle. The divider is only necessary if the laser reference pulse rate is above 40 MHz. Recommendations for setting these values can be found in Appendix A.

The photon count rates were carefully controlled by changing the entrance slit size of the spectrometer and introducing several ND filters. In particular, the PL photon count rate was attenuated to less than one percent of the laser reference pulse rate. The photon count rate in the IRF measurement, however, had to be attenuated even further to account for differential count rate.

Differential count rate is an important consideration in reducing error in the IRF. When collecting data, the TCSPC software displays the count rate of the PMT and the reference pulse in photons per second. When measuring the lifetime of the sample, the PMT count rate is spread out over the entire decay. The PMT receives a high number of photons at the initial peak, and the count decreases exponentially over time. It is expected then that the counts per second are a fair estimate of the number of counts at the half maximum point of the lifetime decay plot. The IRF, however, does not decay over the entire period as the sample lifetime does. It decays quickly, and the majority of the period is void of photons. The photons per second count is therefore only representative of the photons in a tiny fraction of a second. The PMT is blasted with photons for a very short time, but this high density is then averaged against no photons for the remainder of the period. In order to maintain accuracy and ensure that the IRF will have a similar peak photon density as the sample lifetime, it is necessary to match the differential count rates of the sample and IRF rather than the photon per second count rate. Equation. 2.1 describes how to find the differential count rate. In order to determine what counts per second for the IRF will result in the same differential count rate as the PL from the sample, first determine the differential count rate for the sample, then solve Eq. 2.1 for the IRF counts per second (using the IRF FWHM of lifetime decay) to achieve the same differential count rate as the sample.

$$\text{differential count rate} = \frac{\text{counts per second}}{(\text{laser pulses per second})(\text{FWHM of lifetime decay})} \quad (2.1)$$

### 2.5.2 Data Acquisition

In order to verify our data and potentially use computer learning as a way of predicting temperature, the PL spectrum was also recorded for each temperature. The PL spectrum was measured with a photon counter connected to the PMT. A homemade LabVIEW program recorded the photon counts for each wavelength selected by the spectrometer. The scan was done in wavelength steps of 0.775 nm and taken over a range wide enough to clearly see the entire PL peak.

Photoluminescence lifetime data was collected for five minutes for each of the IRF and sample lifetimes while the sample was under vacuum and at a controlled temperature. This collection time was chosen in order to maximize accuracy in the histogram, while avoiding lengthy collection times. The IRF lifetime was taken with the spectrometer set to the laser wavelength (500 nm) and the RhB lifetime with the spectrometer set to the PL wavelength (583 nm). After collecting spectral data and PL lifetime, the PID controller for the cryostat was re-set for a lower temperature and the sample was allowed to come to thermal equilibrium with the cold finger for 30 minutes before starting data collection again. Lifetime data was taken from room temperature, 296.5 K, to 30 K in increments of 30 K. Data was then taken at the lower limit of the cryostat, 16 K.

In order to give the most accurate estimate of PL lifetime, the pulse generator was set to a long delay time (90 ns) in order to simulate a lower frequency laser. This delay in time between each start pulse allowed for the collection of multiple lifetime decay peaks. During data analysis, the lifetime for each of these peaks was averaged together to give a more accurate lifetime.

## 2.6 Issues Encountered

The vast majority of the issues encountered while setting up the experiment and taking data came from the IRF. First, the IRF is prone to becoming misshapen and distorted when the scattered laser light is slightly misaligned, which is often difficult to manage and correct. This can also become a problem in the middle of data collection when the compressor for the cryostat is on, as the alignment will sometimes slowly drift due to movement and the photon counts may become too high or too low. The best solution to this is to insert an ND filter into the optical path and open the slits into the spectrometer wider so small shifts in position will have little effect on the overall alignment into the spectrometer.

Another problem with the IRF is in data analysis. The IRF will often be shifted in time from the sample lifetime. This may be due to the difference in wavelength between the two measurements. The Mathematica file for data analysis, found in appendix C, includes a slider to shift the IRF in time to accommodate this; however, shifting the IRF is not ideal as the difference in counts between the tail end and leading end may differ and introduce error as the IRF is "wrapped" around the time range. The IRF is also shaped differently than the sample lifetime, in particular the first and last decay peaks are always different amplitudes than those of the sample. For this purpose, the Mathematica file includes sliders to select the portion of data for analysis to reduce the error of these peaks. The IRF may display other oddities in terms of shape, and the only sure way to avoid serious error is to complete the data analysis each time data is taken and be sure the IRF is well behaved before moving further with measurements.

# Chapter 3

## Results and Conclusions

### 3.1 Overview

In this chapter, I will discuss the relationship between PL lifetime and temperature for rhodamine B, as well as outliers, and fit a sigmoidal function to the data. I will also give conclusions and further work.

### 3.2 Deconvolution

Deconvolution, a data analysis technique, is a necessary step in determining the PL lifetime of the rhodamine B sample. The raw data measured from the sample is not an accurate representation of the true lifetime. The PMT photon detector does not have an infinitely quick response to a photon and adds a contribution to the lifetime. The PMT response, i.e. the instrument response function (IRF), is convolved with the true PL decay to produce the measured data. Fig. 3.1 shows a single PL decay of the rhodamine B sample. Fig. 3.2 shows the PL decay for the IRF, which although a much faster decay, still has a significant width compared to Fig. 3.1.

The true lifetime must be extracted from the raw data with deconvolution techniques, reversing

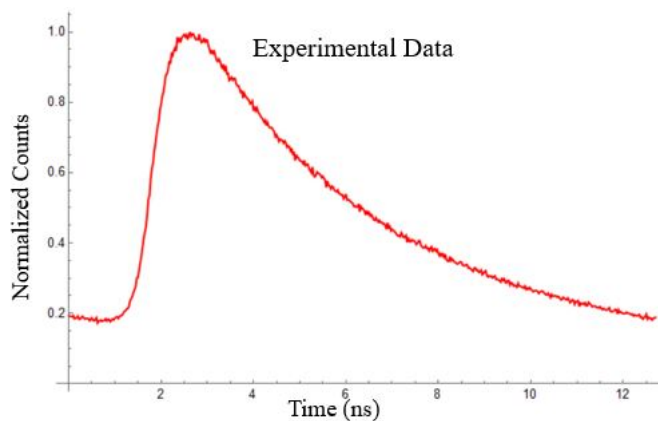


**Figure 3.1** One PL lifetime decay curve for rhodamine B at 296.5 K.

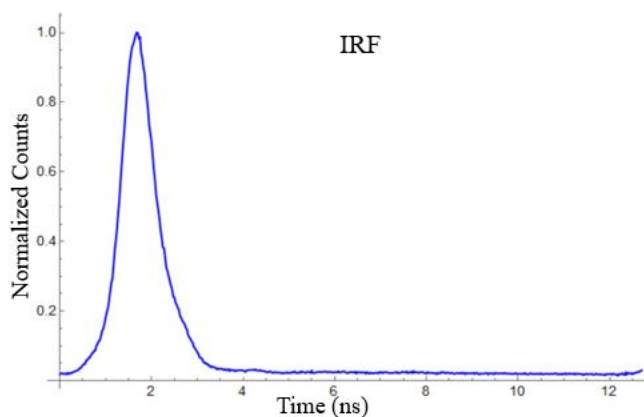


**Figure 3.2** One IRF decay curve at 296.5 K.

the convolution. The difficulty with this process, however, is that the data is inherently noisy and not as well defined as a mathematical function would be. It is therefore almost impossible to simply reverse the convolution using Fourier transforms and the convolution theorem, as the noise in the data, which is not a result of the IRF or the PL of the sample, is impossible to analyze in this way. Instead, iterative reconvolution, a common method in TCSPC data analysis, was used to deconvolve the data [1]. A homemade Mathematica file guessed the accurate lifetime, convolved this guess with the experimental IRF measurement, and compared the result to the raw sample data. The guess was then adjusted and compared again, and the process was repeated until the error between the

guessed convolution and the raw data was minimized. The adjusted guess was then representative of the true lifetime histogram. The lifetime value was then determined as the time it takes for the decay to reach  $1/e$  of the peak amplitude.

Using this method of deconvolution comes with its own issues. Most importantly, guessing the true PL decay requires knowledge of the functional form of the decay. PL decays in TCSPC are one or multiple exponential decays, depending the recombination method and complexity in PL. Rhodamine B was assumed to exhibit a single exponential decay, although this assumption may not always be accurate [9]. Another issue is that the the guessed function is forced to zero at time zero, which is not representative of the actual data and can result in significant error in the first portion of the function. This issue can be avoided by selecting a portion of the data to compare the guess against, essentially ignoring the first error-prone section of the data. Another error comes from a time shift between the IRF measurement and the RhB data. The IRF data must be shifted in time to match the sample measurement by wrapping one edge of the data around to the other edge.

### 3.3 Data

The lifetime versus temperature data for the rhodamine B sample is plotted in Fig. 3.3. As seen, there are a few outliers, particularly at 16 K and 30 K, which were unfortunately unable to be resolved at the time of measurement. The plot of lifetime vs. temperature data was best fitted to a five parameter sigmoidal function, as shown in Fig. 3.3.

The fitted five parameter sigmoid is described as Eq. 3.1, where  $a$ ,  $b$ ,  $c$ ,  $d$ , and  $m$  are fitting parameters. The initial fitting parameters and their respective values for the RhB data are described in Table 3.1 [13].

$$f(x) = b + \frac{c - b}{(1 + (x/a)^d)^m} \quad (3.1)$$

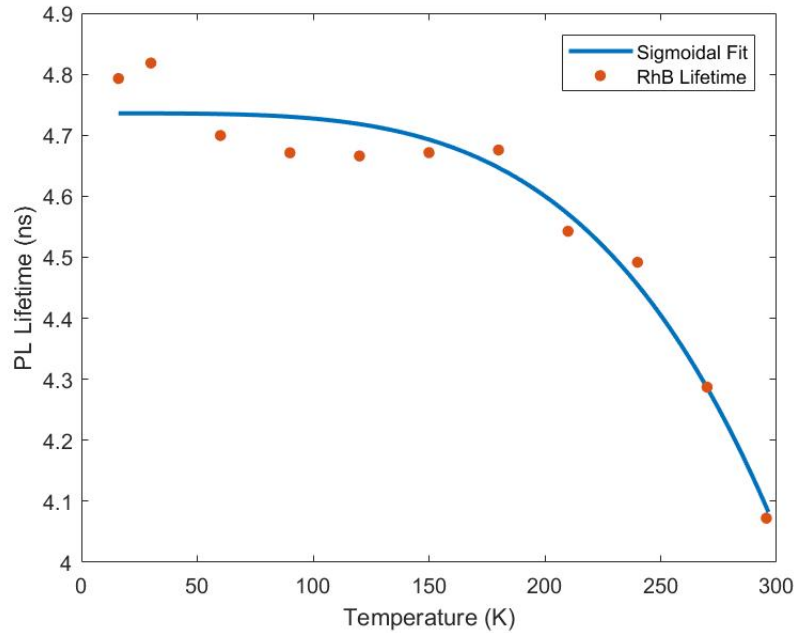


**Figure 3.3** Plot of PL lifetime vs. temperature for rhodamine B. A five parameter sigmoidal function is fitted to the data.

**Table 3.1** Initial fitting parameters for the five parameter sigmoidal function and their values for RhB.

Fitting Parameter	Description	Value
b	minimum asymptote	-652.91
c	maximum asymptote	4.74
a	inflection point	5033.26
d	slope of the curve	3.99
m	asymmetry factor	81.28

This sigmoidal fit is not perfect. Because the data taken in this experiment only fits well with a portion of the s-shaped sigmoidal function, it is impossible to prove that the PL lifetime continues to follow a sigmoidal shape at higher temperatures. Because of this, the parameter b and a cannot be reliably determined. In table 3.1, b was initially determined to be -652.91, implying that the PL

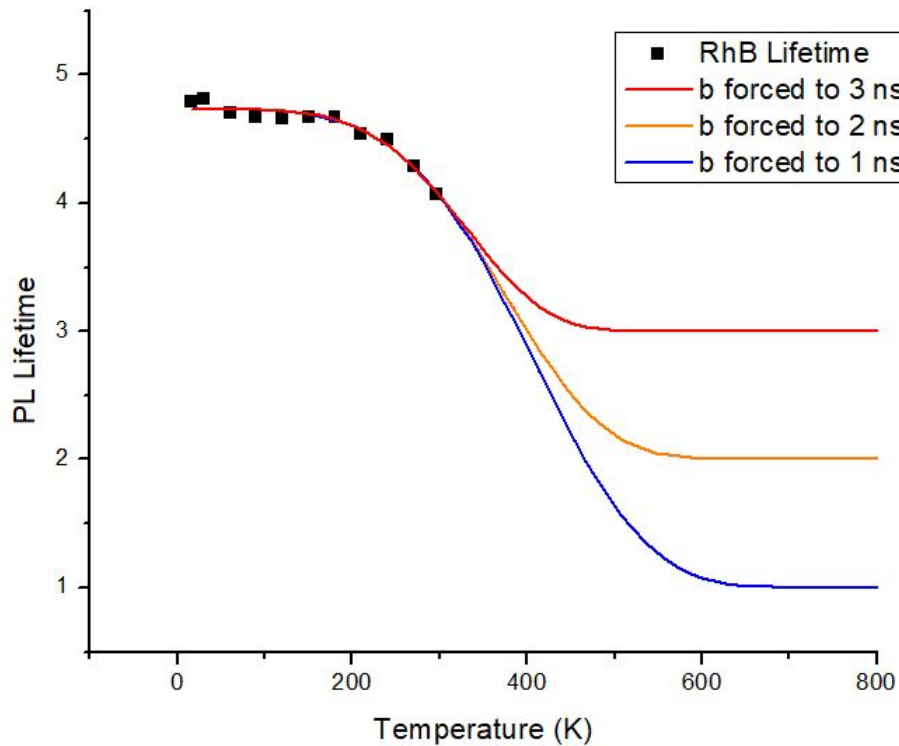


**Figure 3.4** Five-parameter sigmoidal fits with RhB PL lifetime data. The fits are extended beyond the measured temperatures to 800 K. The fitting parameter  $b$  is forced to 1 ns, 2 ns, and 3 ns. Only the inflection point and the minimum asymptote vary.

lifetime does not come to an asymptote again until it reaches  $-652.91$  ns. This is impossible. The behavior can be explained by extending the fit beyond the measured temperatures and forcing  $b$  to be a believable lifetime. Figure 3.4 shows the result of forcing  $b$  to be 1, 2, and 3 ns. For each value of  $b$ , the fit with the measured RhB PL lifetimes remain the same as in Fig. 3.3, but the inflection point (parameter  $a$ ) and minimum asymptote (parameter  $b$ ) vary widely. Without higher temperature measurements, the sigmoidal fit can only be defined near the maximum asymptote. In this region, a sigmoidal function was the best fit found for the RhB PL lifetime data, although whether the fit continues to be sigmoidal at higher temperatures must be proven in future studies.

The behavior of the lifetime vs. temperature can possibly be explained by quenching. Quenching, which is explained in section 1.2, artificially lowers the lifetime of the sample through several

different processes. At low temperatures, dynamic quenching is effectively nonexistent, and the lifetime approaches the intrinsic lifetime of the sample. At higher temperatures, dynamic quenching is introduced, and the lifetime is lowered as more quenching processes occur. Above room temperature, which was not measured in this experiment, quenching is expected to slow and the lifetime to approach an asymptote. This higher temperature asymptotic behavior is shown in a study on RhB in water [5], which supports the conclusion of a sigmoidal fit, although full sigmoidal behavior with two asymptotes has not been proven.

The PL spectra at the measured temperatures is plotted in Fig. 3.5. Photoluminescence intensity does indeed vary with temperature; however, the variations are not consistent between temperatures. Instead the behavior of the intensity at different wavelengths is somewhat erratic, possibly due to small shifts in the optical alignments over time or fluctuations in laser power.

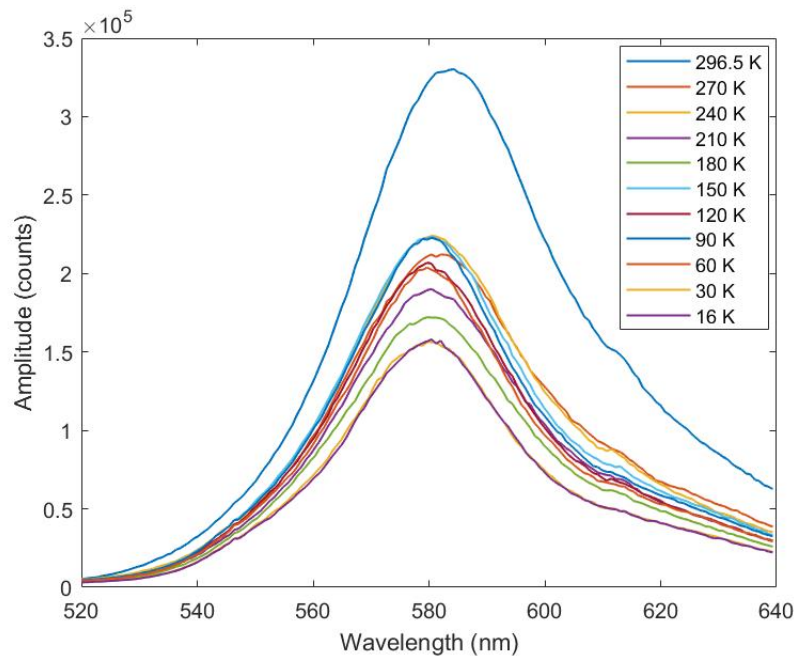


**Figure 3.5** Photoluminescence spectra plotted at the measured temperatures.

## 3.4 Conclusions

Using time-correlated single photon counting, the photoluminescence lifetime of rhodamine B was successfully measured at temperatures ranging from 16 K to 296.5 K. The relationship between PL lifetime and temperature for rhodamine B can be fitted with a sigmoidal function, which behaves as expected due to quenching. Although there were a few unresolved outliers, the data clearly shows the trend in the relationship.

## 3.5 Further Work

The sigmoidal function obtained from the data on rhodamine B can be used as a predictor of temperature for any lifetime within the measured temperature range in future work. Much of the process of collecting lifetime data should be streamlined and better understood for more work on temperature probes; in particular, data collection may be made faster and more efficient, the exact behavior of the IRF should be better understood to reduce errors and imprecise lifetime measurements, and the deconvolution method can be made to run faster and minimize introduced errors.

In order to complete the analysis of rhodamine B, PL lifetime will be taken at a few temperatures above 300 K in order to verify the behavior of the sigmoidal function. Machine learning may also be used for better predictions of temperature from PL lifetimes and PL spectra.

After rhodamine B, the same process will be used to determine the temperature dependence of the lifetime of other materials, such as cadmium telluride (CdTe) quantum dots. These materials will also be used in production of temperature sensors for microfluidic devices.

# Appendix A

## TCSPC Settings

Accurate settings for the Picoquant PICO TimeHarp 260 module are important for efficient data collection and filtering data. The settings for the Picoquant PICO model TimeHarp 260 are zero cross level, discriminator level, offset, sync divider, resolution, acquisition time, and mode. Both the sync channel (laser reference pulse) and the input channel (PMT pulse) have settings for the zero cross, discriminator, and offset.

The TCSPC software will display two modes, oscilloscope mode and integration mode. Oscilloscope mode will continuously collect lifetime data in set time increments and may be useful in small adjustments prior to data acquisition. Integration mode is used for data acquisition. In this mode, lifetime data is collected over the acquisition time and does not repeat.

To set the zero cross and discriminator levels for the sync channel, check with an oscilloscope that the sync signal is within safe voltage levels (not exceeding -1.2 V). The TimeHarp will only accept negative voltage signals. Ideal values for amplitude are between -100 mV and -200 mV. Make sure the rising edge is less than 2 ns. Set the zero cross level to 10 mV. The discriminator level should be set to half the amplitude of the sync pulse.

The input channel levels should be set in the same way as the sync channel. Verify that the pulses are within the voltage limits. Set the zero cross level to 10 mV and the discriminator level to

half the expected pulse amplitude.

The offset should be initially set to zero. When taking data, if the histogram needs to be shifted in time, set the offset to a significant value (1e5 ns) and adjust.

The sync divider is used to ensure that the TCSPC module does not have to process sync frequencies above 40 MHz. If the sync rate is larger than 40 MHz, implement a larger sync divider until the resulting rate is below 40 MHz. The sync divider can be set to 1, 2, 4, or 8. Using the pulse generator to lower the start pulse rate is a way of avoiding using a divider higher than 1, as was done in the RhB experiment by lowering the 80 MHz laser pulse to 10 MHz with a long delay.

# Appendix B

## PID Controller

Taking temperature-sensitive data required maintaining a constant temperature accurately. The cryostat temperature is controlled by a PID temperature controller connected to a heater. As the compressed helium cools the cryostat down, the heating element turns on and off to maintain a set temperature. How the heating element is regulated, how much fluctuation is present around the set temperature, and how fast the temperature converges on the set value is dependent on the PID values. In order to be confident in the speed, accuracy and stability of the temperature in the cryostat, I experimentally determined the values for PID settings at temperatures from 300K (room temperature) to 16K (lowest temperature possible). Changing these settings for each temperature must be done manually.

**Table B.1** Input values at different temperatures for the proportion (P), integral (I), and derivative (D) values for the PID temperature controller

Temperature (K)	P	I	D
300	50	20	2
275	50	20	2
250	50	20	2
225	55	20	3
200	55	20	3
175	55	20	3
150	65	20	3
125	65	20	3
100	70	20	3
75	70	20	3
50	70	20	4
25	75	20	6

# Appendix C

## Data Analysis Code

This appendix contains the Mathematica file used for the iterative reconvolution data analysis technique. Sample and IRF data must be taken with the same time scale, offset, and length. Data files must be comma-separated value files (.csv). IRF data is imported to "irf2column" and sample data to "measured2column".

The first section of the code imports the data and sets up a manipulate plot to adjust the guessed lifetime plot to match the measured data and start the iteration process with values close to the final result. The manipulate plot will adjust the starting "guessed" amplitude, slope, and time shift. It also allows the selection of data that will be exclusively analyzed by highlighting the desired data region and excluding data outside the highlight from the result.

The second section of the code iterates the guess until the error is minimized. The measured data and the result of the iterative convolution are plotted together for a visual representation of the error, and the final lifetime is given.

```
(* This assumes the IRF and data files were taken under identical conditions,  
namely they have the same time scale (start, stop, and spacing)  
and had the same laser pulse onset (no t0 offset) *)
```

```
Clear["`*"]
```

```
SetDirectory[NotebookDirectory[]];
```

```
irf2column = Import["irf_file.csv"];
```

```
measured2column = Import["rhb_file.csv"]; (* x-values must agree with IRF *)
```

```
times = Transpose[irf2column][[1]];
```

```
tmin = times[[1]];
```

```
times = times - tmin;
```

```
(* force time to start at 0, not sure if really needed *)
```

```
tmin = 0;
```

```
tmax = times[[-1]];
```

```
(*pitch=times[[2]]-times[[1]];*)
```

```
pitch = 0.025;
```

```
numpoints = Length[times]; (* if you care *)
```

```
plot[functionname_String] :=
```

```
ListLinePlot[Transpose[{times, ToExpression[functionname]}],  
PlotRange -> All, PlotLegends -> functionname]
```

```
irf = Transpose[irf2column][[2]];
```

```
irf = irf / Total[irf]; (* normalize by "area" *)
```

```
plot["irf"]
```

```
measured = Transpose[measured2column][[2]];
```

```
measured = measured / Max[measured]; (* normalize by amplitude *)
```

```
plot["measured"]
```

```
(* "guess" is the function that I'm trying to deduce,
```

```
by fitting the convolution of "guess" with
```

```
"irf" (called "convolved") to match the measured data.
```

```
*)
```

```
Print[
```

```
"-----"]
```

```
guess[a_, tau_] := Table[a Exp[-t / tau], {t, tmin, tmax, pitch}]
```

```
plot["guess[1,10]"]; (* just a representative plot *)
```

```
convolved[a_, tau_] := a Rescale@ListConvolve[irf, guess[a, tau], 1, 0]
```

```
plot["convolved[1,10]"]; (* just a representative plot *)
```

```

Print[
  "-----"
  (* this allows the user to get good starting values. *)
Manipulate[ListLinePlot[{{times,
  RotateRight[measured, Round[measuredshiftinit * numpoints / (tmax - tmin)]]} //
  Transpose, {times, convolved[ainit, tauinit]} // Transpose},
  PlotRange -> All, ImageSize -> Large,
  Epilog -> {{Blue, Opacity[0.1], Rectangle[{tleft, 0}, {tright, 1.1}]}}],
{ainit, 0.9, 1.1}, {tauinit, 0.5, 20},
{measuredshiftinit, -(tmax - tmin) / 20, + (tmax - tmin) / 20, pitch},
{tleft, tmin, tmax}, {tright, tmin, tmax},
LocalizeVariables -> False, SaveDefinitions -> True]

(* this prints the final values of the
  fit obtained from the Manipulate command *)
Print["a init"]
ainit
Print ["tau init"]
tauinit
Print ["measured shift init"]
measuredshiftinit
Print["tleft"]
tleft = Min[tleft, tright]
Print ["tright"]
tright = Max[tleft, tright]
startpoint = Round[(tleft - tmin) / pitch];
(* the point number corresponding to tleft *)
endpoint = Round[(tright - tmin) / pitch];
(* the point number corresponding to tright *)

(* this defines the error function for the minimization,
  as a function of the two parameters *)
Print[
  "-----"
  -----"]
errornoncompiled[a_, tau_, measuredshift_] :=
  Total[ ((convolved[a, tau] - RotateRight[measured, Round[
    measuredshift * numpoints / (tmax - tmin)]] ) ^2) [[startpoint ;; endpoint]] ]
error = Compile[{{a, _Real}, {tau, _Real}, {measuredshift, _Real}},
  errornoncompiled[a, tau, measuredshift],
  "RuntimeOptions" -> {"EvaluateSymbolically" -> False}];

```

```

(*Print["error"]
  errornoncompiled[1,1];
(* just a couple of test values to make sure it's working *)
error[1,1]; *)

(* to help visualize the minimum of the error function *)
Print[
  "-----"
  "-----"]
Plot[error[a, tauinit, measuredshiftinit],
  {a, .9 ainit, 1.1 ainit}, PlotLabel -> "tau error"]
Plot[error[ainit, tau, measuredshiftinit],
  {tau, 0.9 tauinit, 1.1 tauinit}, PlotLabel -> "a error"]
Plot[error[ainit, tauinit, measuredshift],
  {measuredshift, -(tmax - tmin) / 20, + (tmax - tmin) / 20},
  PlotLabel -> "measured shift error"]

Print[
  "-----"
  "-----"]
params = FindMinimum[error[a, tau, measuredshift], {{a, ainit}, {tau, tauinit},
  {measuredshift, measuredshiftinit}}, Method -> "PrincipalAxis"] // Last ;
ListLinePlot[guess[a /. params, tau /. params], PlotRange -> All,
  PlotLegends -> "answer" <> ToString[params]]
ListLinePlot[convolved[a /. params, tau /. params],
  PlotRange -> All, PlotLegends -> "convolved"];
ListPlot[{RotateRight[measured,
  Round[(measuredshift /. params) * numpoints / (tmax - tmin)]],
  convolved[a /. params, tau /. params]}, DataRange -> {tmin, tmax},
  PlotStyle -> {Directive[PointSize[0.005], Black],
  Directive[Thickness[0.015], Darker@Green]}, Joined -> {False, True},
  PlotLegends -> "measured data (black pts) and fitted convolved (green line)",
  PlotRange -> All, ImageSize -> Large,
  Epilog -> {{Blue, Opacity[0.1], Rectangle[{tleft, 0}, {tright, 1.1}]}}]

```

# Index

Avalanche photodiode, 11

Common fraction discriminator, 6

Converters

- Analog-to-digital, 6
- Time to digital, 10
- Time-to-amplitude, 6

Cryostat, 14

Dead time, 7

Deconvolution, 18

Differential count rate, 15

Instrument response function, 9

Photoluminescence, 2

Photomultiplier tube, 13

Pile-up, 9

Pulse generator, 12

Quantum yield, 3

Quenching, 3, 22

Rhodamine B, 4

TCSPC modes

- Forward, 9
- Reverse, 9

Time-correlated single photon counting, 5

Zero cross level, 7

# Bibliography

- [1] W. Becker, A. Bergmann, M. A. Hink, K. König, K. Benndorf, and C. Biskup, “Fluorescence lifetime imaging by time-correlated single-photon counting,” *Microscopy Research and Technique* **63**, 58–66 (2004).
- [2] Picoquant, *TimeHarp 260 user’s manual and technical data*.
- [3] C. Paviolo, A. H. A. Clayton, S. L. McArthur, and P. R. Stoddar, “Temperature measurement in the microscopic regime: a comparison between fluorescence lifetime- and intensity-based methods,” *Journal of microscopy* **250**, 179–188 (2013).
- [4] D. Wong, “Fluorescence and Phosphorescence,” [https://chem.libretexts.org/Core/Physical\\_and\\_Theoretical\\_Chemistry/Spectroscopy/Electronic\\_Spectroscopy/Fluorescence\\_and\\_Phosphorescence](https://chem.libretexts.org/Core/Physical_and_Theoretical_Chemistry/Spectroscopy/Electronic_Spectroscopy/Fluorescence_and_Phosphorescence) (Accessed 2018).
- [5] P. Sanvito, “Quenching of fluorescence with temperature,” Technical report, Edinburgh Instruments (2016) .
- [6] M. Brandt, “Quenching Processes,” 1999.
- [7] X. dong Wang, O. S. Wolfbeis, and R. J. Meier, “Luminescent probes and sensors for temperature,” *Chem. Soc. Rev.* **42**, 7834 (2013).

- 
- [8] M. Y. Berezin and S. Achilefu, "Fluorescence Lifetime Measurements and Biological Imaging," *Chemical reviews* **110**, 2641–2684 (2010).
- [9] R. Mercade-Prieto, L. Rodriguez-Rivera, and X. D. Chen, "Fluorescence lifetime of Rhodamine B in aqueous solutions of polysaccharides and proteins as a function of viscosity and temperature," *Photochemical and Photobiological Sciences* **16**, 1727–1734 (2017).
- [10] D. Magde, G. E. Rojas, and P. G. Seybold, "Solvent dependence of the fluorescence lifetimes of xanthene dyes," *Photochemistry and photobiology* **70**, 737–744 (1999).
- [11] R. F. Kubin and A. N. Fletcher, "Fluorescence quantum yields of some rhodamine dyes," *Journal of Luminescence* **27**, 455–462 (1982).
- [12] t. f. e. Wikipedia, "Operation of a CFD," 2013.
- [13] G. Cardillo, "Five parameters logistic regression - There and back again," 2012.

# Index

Avalanche photodiode, 11

Common fraction discriminator, 6

Converters

- Analog-to-digital, 6
- Time to digital, 10
- Time-to-amplitude, 6

Cryostat, 14

Dead time, 7

Deconvolution, 18

Differential count rate, 15

Instrument response function, 9

Photoluminescence, 2

Photomultiplier tube, 13

Pile-up, 9

Pulse generator, 12

Quantum yield, 3

Quenching, 3, 22

Rhodamine B, 4

TCSPC modes

- Forward, 9
- Reverse, 9

Time-correlated single photon counting, 5

Zero cross level, 7